Analysis of Transients and Semi-Conductors

P. Godkhindi
Data Recorder, Editor

C. Lin
Data Analyst, Circuit Specialist

K. Thomas
Editor, Notebook Writer

N. Vadivelu
Data Analyst, MATLAB Specialist

(Received by 23 November 2016)

Through the use of three circuits, the behaviours of a 10 μF capacitor, a 1N5818 PN junction diode, and an BC547B NPN transistor were determined. The capacitor had a charging curve of $q_C(t) = (49.50 \pm .07)(1 - e^{-t(0.263 \pm .003)^{-1}})$ μC and a discharging curve of $q_D(t) = (44.96 \pm .09)\ e^{-t(0.294 \pm .001)^{-1}}$ μC. The diode's electric potential and current in forward bias were related through the equation $i_D(V_D) = (3.2 \pm .2)(e^{\frac{V_D}{(0.0432 \pm .0002)}} - 1)\ \mu A$. The transistor's saturation was reached for base currents 3.5, 10.3, 18.2, and 25.9 μA. It was determined that the transistor had a β-value of (246.02±.03) and an ideality factor of (1.91±.02).

I Introduction

The behaviours and utilities of capacitors, diodes, and transistors were studied through circuits and mathematical modelling.

II Theory

The potential, current, and resistance of a circuit can be related using Ohm's Law:

$$V = iR \qquad [1]$$

(Halliday, 2011)

Where:

V = electric potential difference (V)
i = electric current (A)
R = electric resistance (Ω)

The diode current is given by the Shockley diode equation:

$$I_D = I_S(e^{-\frac{V_D t}{n V_T}} - 1) \qquad [2]$$

(Electronics Tutorials[1], 2016)

Where:

i_D = current through diode (A)
i_S = reverse bias scale current (A)
V_D = potential across diode (V)
V_T = thermal potential (V)
n = ideality factor

The current gain of an NPN transistor is given by the following:

$$\beta = \frac{i_C}{i_B} \qquad [3]$$

(Electronics Tutorials[2], 2016)

Where:

β = current gain
i_C = current through collector (A)
i_B = current through base (A)

Capacitance is given by the following:

$$C = \kappa \frac{q}{V} \qquad [4]$$

(Halliday, 2011)

Where:

C = capacitance (F)
κ = dielectric constant
q = charge (C)

The q through a charging capacitor in a resistor-capacitor (RC) circuit is:

$$q_C(t) = \frac{CV_B}{k}(1 - e^{-\frac{t}{RC}}) \qquad [5]$$

(Halliday, 2011)

Where:

q_D(t) = charge of charging capacitor (C)

For a discharging capacitor in the same circuit:

$$q_D(t) = \frac{CV_B}{k} e^{-\frac{t}{RC}} \qquad [6]$$

(Halliday, 2011)

Where:

q_D(t) = charge of discharging capacitor (C)

RC (τ) is known as the "time capacitance." A capacitor in an RC circuit should have a charge and discharge period of 5τ.

To address the issue of the unknown potential, resistance, or current of circuit components, Kirchhoff's Voltage and Current Laws were applied. These state that the total potential of a closed circuit is always zero, and that the total current of a junction is always zero (Halliday, 2011).

Uncertainty calculations and conventions were followed as outlined by van Bemmel (2016).

III METHOD

All three circuits were set up on a breadboard. To aid in the setup of the circuits, an experimenter board that converted AC to 5 V of DC was used. A Vernier LabQuest, its matching voltmeters, and a digital ammeter completed the experiment's measurements. The voltmeter took readings between 0 to 6 V.

To ensure reliable readings, multimeter and the Vernier voltmeter was verified by measuring the electric potential of several new batteries with known values for their potentials. The Vernier voltmeter was deemed accurate. The multimeter was then used to obtain the precise resistances of the resistors used.

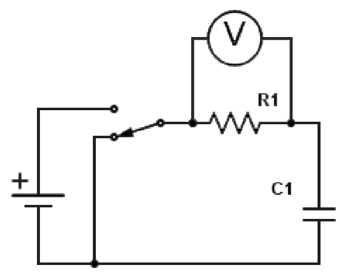

Fig. 1 - RC Circuit Schematic: The circuit above was used in the RC circuit analysis. The switch is in its discharging position in the diagram.

Figure 1 consisted of a 32 kΩ resistor, and a 10 μF axial capacitor. In order to obtain readings, a voltmeter was connected parallel to the resistor, R_1. To avoid erroneous readings, the meter was not connected across the capacitor. As capacitors approach their full charge, they behave like a large resistor, prompting a significant amount of the current to flow into the parallel circuit through which a voltmeter is attached. As the resistance of the capacitor and the voltmeter become more and more similar, the voltmeter's parallel circuit fails to prevent current flow through it. A lower current flow through the capacitor will cause a lower, and more inaccurate, potential reading. However, because the resistance of the resistor remains both constant, and significantly lower than the voltmeter's resistance, such a circuit will not yield erroneous readings.

The circuit was first connected, and the capacitor charged while the voltmeter collected readings. The capacitor was then discharged, and the voltmeter took readings 60 times each second. This frequency was chosen because it optimized the readings and created a smooth curve. Frequencies greater than 60 Hz resulted in oscillatory data caused by discontinuous potential readings.

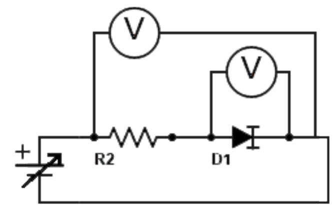

Fig. 2 - PN Diode Circuit Schematic: The circuit above was used in the PN diode circuit analysis. The diode is currently in forward bias, and the reverse orientation would yield a reverse bias.

Figure 2 was used for the PN diode analysis. It used a variable potential source, which ranged from 0 to 6 V. A 1N5818 diode was connected in series with a 10 kΩ resistor and the power source to obtain the required data values in both reverse and forward bias. Voltmeters were connected in parallel to both the entire circuit, and just the resistor. For analysis of the thermal potential in the Shockley diode equation, the temperature of the room was also measured using a thermometer. The deviation in the diode's actual temperature from the room temperature was deemed to be negligible in the determination of the ideality factor.

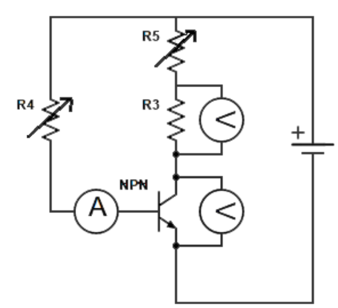

Fig. 3 - Transistor Circuit Schematic: The circuit above was used in the transistor analysis. Two voltmeters were used for the data collection, and the ammeter was removed from the circuit once the base current was determined.

Finally, a BC547B NPN transistor was analyzed. One voltmeter was placed in parallel with the resistor at the collector, and one across the collector and emitter of the transistor, measuring the V_C and V_{CE}, respectively. i_B was changed by varying the resistance of R_4 to obtain currents of 3.5, 10.3, 18.2, and 25.9 μA. An ammeter was used to measure I_B. When the experimenter board's 5 V ran through the entire circuit, the variable resistor before the collector was changed to vary V_{CE}.

IV Data

The Logger Lite software stored the Vernier voltmeter data in a table and presented the data in a graph. For example, Figure 4 shows the potential of the resistor in the RC circuit during charge and then discharge for the fifth RC run.

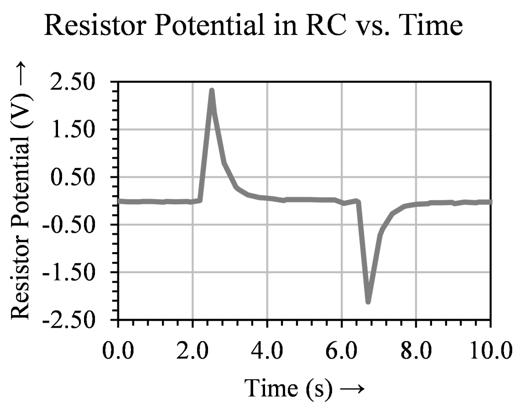

Fig. 4 - Electric Potential of Resistor in RC Circuit vs. Time: The above raw data was collected by the LabQuest. The resistor's electric potential changed during the capacitor charges and discharges. The resistor's potential was used to calculate the capacitor's potential during analysis.

V Analysis

Because the potential across R_1 and the potential across the power source were known, the potential of the capacitor could be determined using Kirchhoff's Voltage Law. Using [4], the capacitor's charge could be calculated for each data point. The capacitance value provided on the packaging for the capacitor already included the effects of the dielectric.

The equation for the capacitor while charging was regressed to be:

$$q_C(t) = (49.50 \pm .07)\left(1 - e^{-\frac{t}{(0.263\pm.003)}}\right) \mu C \quad [7]$$

The equation for the discharge of the capacitor was regressed to be:

$$q_D(t) = (44.96 \pm .09)\, e^{-\frac{t}{(0.294\pm.001)}} \mu C \quad [8]$$

The function for the charge of the capacitor over time, for both the capacitor's charge and discharge, were graphed.

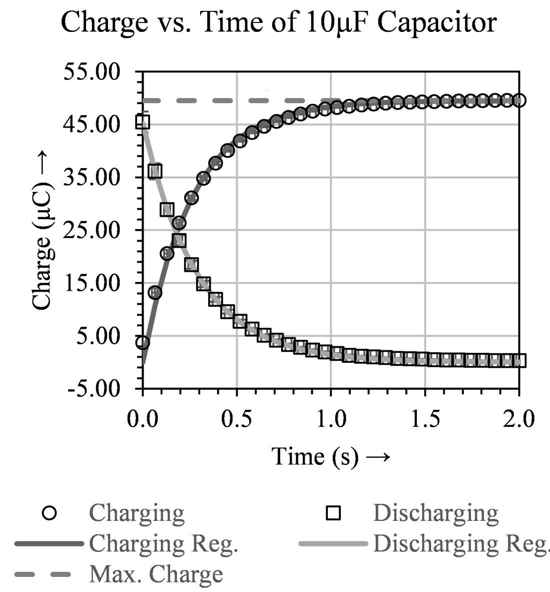

Fig. 5 - Charge vs. Time of a 10 uF Capacitor: From the calculated charge of the capacitor over time, the above charging and discharging curves were determined. Only one fifth of the points are shown for clarity.

As expected from theory, [7] and [8] have similar coefficients in front of e and $-t$. It is known from [5] and [6] that the coefficients for the charging and discharging curves have the same parameters: C, V_B, R, and k. Because these values remain the same for the charge and discharge functions, the curves are symmetrical. When the capacitor charges, it approaches $\frac{CV_B}{k}$. When the capacitor discharges, it begins at $\frac{CV_B}{k}$ and approaches zero in a manner that is the reverse of the charging curve.

$\frac{CV_B}{k}$ was the coefficient before both the charging and discharging functions. It was predicted to be 50 μC using known capacitance, battery potential values. The values that were experimentally regressed were

(49.50±.07) for charging and (44.96±.09) for discharging. It was theorized that the discharging graph had a greater discrepancy from the predicted values beause of the residual potential in the wires.

The time capacitance value (τ) was theorized to be 0.32 using the resistor and capacitance values. It was calculated as the factor dividing t: (0.263±.003) for charging and (0.294±.001) for discharging.

Because a full charge or discharge elapsed a time of roughly 1.5 s (5τ), the RC circuit confirmed the established theory once again.

The capacitors charged and discharged in this fashion due to the buildup of electrons. As they charged, the increasing amount of electrons created an increasingly repulsive electromagnetic force against incoming electrons. This causing the slowing curve observed. Conversely, during discharge, the decreasing number of electrons created a decreasingly repulsive electromagnetic force against stored electrons, causing the observed shallowing curve.

For the PN diode circuit, the variable power source provided a potential over the resistor and the diode. Two voltmeters gave the potential across the resistor and across the entire series circuit. With these values, Kirchoffs Laws were used to find the potential of the diode. The resistance and potential of the resistor were used to determine the circuit current. It was impossible to obtain potentials nearing 0 V due to residual potential in the wires, and lack of equipment sensitivity.

The V-i data for the PN diode was regressed, yielding [9]. It was noted that Shockley's Diode equation was applicable to all potential values between the diode's reverse and forward breakdowns.

$$i_D(V_D) = (3.2 \pm .2)\,(e^{\frac{V_D}{(0.0432\pm.0002)}} - 1)\ \mu A \qquad [9]$$

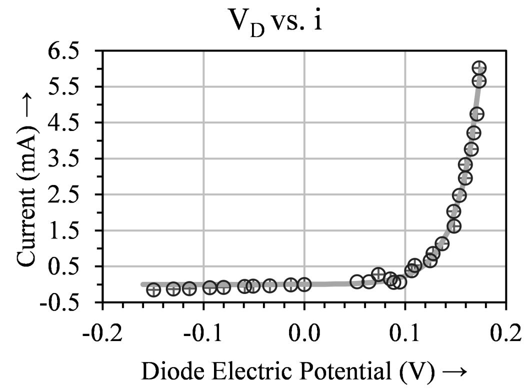

Fig. 6 - Potential vs. Current of a PN Diode: The following data was achieved during the analysis of the PN Diode circuit. The negative potentials were achieved when the diode was in reverse bias, while the positive potentials were achieved in forward bias. Only one fifth of the points are shown for clarity.

The negative potentials were achieved through reverse bias, and the result was linear until breakdown at -0.2 V.

Because diode restrict the flow of current to one direction, the reverse bias trend was theorized to be close to 0 V and to have a small slope. Perfect diodes only exist theoretically, however, which is why the potential remained slightly negative. Furthermore, after -0.2 V, the diode reached its reverse bias breakdown point, and began dropping lower. The current then began leaking severely.

[9] and its coefficients were compared to the predicted values. The PN diode circuit was simulated on the LT Spice Circuit Simulator, yielding the potential vs. current graph. The simulated regression was:

$$i_{D,s}(V_D) = (3.54 \pm .05)\,(e^{\frac{V_D}{(0.0364\pm.0001)}} - 1)\ \mu A \qquad [10]$$

Where:
$i_{D,s}$ = simulated diode current (A)

i_S, also known as the diode saturation current, quantified the current that leaked through the diode in the opposite direction. It was characteristic to the diode, and from the experimental regression, i_S was (3.2±.2) μA. Comparatively, the simulated value for i_S was (3.54±.05) μA. The minor discrepancy was attributed to the air-filled environment around the diode.

The value that divided V_D in both equations was the product of V_T, and the ideality factor, n. This divisor was found to be (0.0432±.0002) experimentally, and (0.0364±.0001) via simulation. When comparing the two, the temperature was set at a constant (296.0±.7) K, which was the room temperature measured during data collection. Based on sourced values for the Boltzmann constant and the elementary charge, the ideality factor was calculated to be (1.91±.02) experimentally and (1.43±.01) by simulation. Ideality factors are normally between 1 and 2, supporting the obtained value. Diodes of the calibre used in this experiment would not be perfectly efficient. There must have existed a factor that altered the ideal diodes V-i graph to suit the non-ideal situation.

For the analysis of the transistor, the current through the transistor's collector, calculated using the measured electric potential, was graphed against the potential across the transistor's collector-emitter. A curve was obtained for each of the four base currents. The trend lines obtained from the transistor's LT Spice simulation were plotted on the graph for comparison. It was concluded that the simulated data was similar to the experimental data and supported the theory, especially when considering the quality of the equipment.

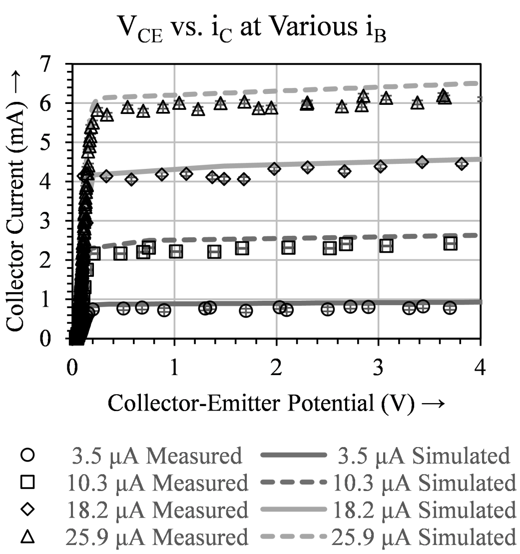

Fig. 7 - Collector-Emitter Potential vs. Collector Current at Varying Base Currents: The potential across the transistor's collector and emitter was plotted against the collector's current. Four base currents were used in the analysis. The results of the LT Spice Circuit Simulator were graphed for comparison. Only a few representative data points are shown.

As the base current increased, the saturation point of the curve was reached with lower collector-emitter potential. Yet, the collector current was much higher as the base current increased. This made sense because a greater base current translated into greater current amplification in the collector-emitter circuit.

When each base current graph leveled out, the saturation point of the curve was reached. Here, collector current became independent of collector-emitter potential. Therefore, the base current no longer amplified the current of the collector-emitter.

Using [3], a beta value was found for each base current with a data point on its curve that was past its saturation point. This beta value was averaged to be (246.02±.03). This value was indicative of the NPN transistors capability of amplifying current. From a given base current, the current of the collector could be up to 250 times the base current. Prior to the saturation point of each curve, the beta value of the transistor would be less.

For all three of the analyzed components, the observed-calculated residuals remained under 15.71%.

VI Sources of Error

The most significant source of error within this experiment was the fact that the circuits did not operate within a vacuum. The ions in the surrounding air slightly affected the operation of every circuit.

In addition, residual potential of the wires caused issues in the RC circuit and diode circuit analyses. In the RC circuit, the residual potential meant that the capacitor was unable to reach full discharge. This skewed the values of the $q_D(t)$ regression. For the diode circuit, because the potentials of the circuit would not drop below 0.1 V the voltmeter was unable to sense any potentials that were close to zero. Consequently, Figure 6 lacked data points near its centre.

VII Conclusion

From the three circuits analyzed, the mathematical relationships of each circuit was determined. For the RC circuit, the capacitor had a charging curve of $q_C(t) = (49.50 \pm .07)(1 - e^{-\frac{t}{(0.263\pm.003)}})\ \mu C$

and discharging curve of $q_D(t) = (44.96 \pm .09)e^{-\frac{t}{(0.29\pm.001)}}\ \mu C$. The diode circuit produced a V-i graph of $i_D(V_D) = (3.2 \pm .2)(e^{\frac{V_D}{(0.0432\pm.0002)}} - 1)\ \mu A$. Finally, the transistor's V_{CE} and i_C were plotted; a β value of (246.02±.03) and an ideality factor of (1.91±.02) were found. With negligible error, all circuits supported their accepted theories.

VIII Sources

van Bemmel, H., Handling of Experimental Data, Marc Garneau C.I. Physics Dept., 2016

[1]*Electronics Tutorials, Diodes, Electronics Tutorials Online, 2016.*

[2]*Electronics Tutorials, Transistor Circuits, Electronics Tutorials Online, 2016.*

Halliday & Resnick, Fundamentals of Physics 9th Ed, 2011